CROATICA CHEMICA ACTA CCACAA **74** (3) 529–544 (2001)

ISSN-0011-1643
CCA-2748

Original Scientific Paper

Structure and Reactivity of $(PPh_4)_3[W(CN)_5O] \cdot 7H_2O$. Kinetics and Mechanism of the Reaction with Molecular Oxygen*

Janusz Szklarzewicz,[a] *Dariusz Matoga,*[a] *Alina Samotus,*[a,**] *John Burgess,*[b] *John Fawcett,*[b] *and David R. Russell*[b]

[a]*Faculty of Chemistry, Jagiellonian University, R. Ingardena 3, 30-060 Kraków, Poland*

[b]*Department of Chemistry, University of Leicester, Leicester LE1 7RH, UK*

Received June 12, 2000; revised August 22, 2000; accepted September 26, 2000

The $(PPh_4)_3[W(CN)_5O] \cdot 7H_2O$ has been synthesised and structurally characterised by X-ray diffraction. In the solid state and in ethanol-acetone mixture, the salt reacts with molecular oxygen giving $(PPh_4)_2[W(CN)_4O(O_2)]$. The progress of the solid state reaction was followed by measuring infrared spectra. The integrated intensities of the W=O, O–O and C≡N bands changed with time according to the pseudo first-order kinetics. In solution, the kinetic measurements indicate that the rate law is of the form $-d[complex]/dt = k[complex][O_2]$. The k value is equal to 5.78 (±0.26) mol^{-1} dm^3 s^{-1} at 298 K. The activation parameters, $\Delta H^{\ddagger}$ (k) and $\Delta S^{\ddagger}$ (k), are 55 (±3) kJ mol^{-1} and –46 (±8) J K^{-1} mol^{-1}, respectively. A reaction mechanism is proposed.

Key words: Oxopentacyanotungstate(IV), oxoperoxotetracyanotungstate(VI), reaction with dioxygen, kinetics and mechanism.

INTRODUCTION

During the last decade, a series of oxo-cyano complexes of molybdenum(IV) and tungsten(IV) with various monodentate ligands of formula

---

* Dedicated to Professor Smiljko Ašperger on the occasion of his 80th birthday.

** Author to whom correspondence should be addressed. (E-mail: samotus@chemia.uj.edu.pl)

$[M(CN)_4O(L)]^{n-}$, where L = NCS^-, N_3^-, F^-, HCN and py (pyridine), M = Mo or W have been synthesised and characterised.[1–3] The only member that has so far been found to react with dioxygen was the anhydrous salt, $(PPh_4)_3[Mo(CN)_5O]$ (L = CN^-), which in aerated CH_2Cl_2 solution gave the peroxo compound, $(PPh_4)_2[Mo(CN)_4O(O_2)]$. The latter salt was isolated and structurally characterised.[4] It was found that the hydrated analogue, $(PPh_4)_3[Mo(CN)_5O] \cdot 7H_2O$, was unreactive towards molecular oxygen.[5] To explain this fact, it was suggested that the presence of water molecules, which formed a network of hydrogen-bonds around the complex anion, eliminated the possibility of dioxygen uptake.

Recently, we have found other complexes of the $[M(CN)_4O(L)]^{n-}$ type, with L = pyrazine (pz), which are reactive towards molecular oxygen despite the presence of water molecules.[6] For M = Mo, the reaction product was found to have the formula $(PPh_4)_2[Mo(CN)_4O(O_2)]$ and its crystal structure was found to be nearly identical to that of the salt obtained from $(PPh_4)_3[Mo(CN)_5O]$.[4] It seems interesting to check whether $(PPh_4)_3[W(CN)_5O] \cdot 7H_2O$ is reactive towards molecular oxygen and if so to determine, as far as possible, the kinetics and mechanism of the reaction with dioxygen.

EXPERIMENTAL

Materials

The $K_3Na[W(CN)_4O_2] \cdot 6H_2O$ was synthesised by the reduction of $Na_2WO_4 \cdot 2H_2O$ with $NaBH_4$ in the presence of KCN as described earlier.[7] All other solvents and reagents were of analytical grade (Aldrich) and used as supplied.

Syntheses

*$(PPh_4)_3[W(CN)_5O] \cdot 7H_2O$ (**1**)*

To a solution of $K_3Na[W(CN)_4O_2] \cdot 6H_2O$ (2 g, 3.6 mmol) in 50 cm^3 of H_2O, titrated with 3 mol dm^{-3} HCl to reach pH *ca.* 7.5, solid KCN (0.23 g, 3.6 mmol) and $(PPh_4)Cl$ (5 g, 12.5 mmol) were added. The mixture was left for two days and the resulting dark green crystals were filtered off, washed with distilled water and dried in air. Yield *ca.* 99%. Selected IR bands (KBr) ν_{max}/cm^{-1}: ν(W=O) 965vs; ν(C≡N) 2099vs, 2115w. Reflectance spectrum ($BaSO_4$): 430 and 660 nm.

Anal. Calcd. for $C_{77}H_{74}N_5O_8P_3W$: C, 62.68; N, 4.75; H, 5.02; H_2O, 8.55%. Found: C, 62.46; N, 4.58; H, 4.73; H_2O, 8.70%.

*$(PPh_4)_3[W(CN)_5O]$ (**2**)*

The anhydrous salt **2** was synthesised by thermal (at 323 K) or by vacuum dehydration of salt **1** (over P_4O_{10}). Selected IR bands (KBr) ν_{max}/cm^{-1}: ν(W=O) 917vs; ν(C≡N) 2060vs, 2068vs, 2098w. Reflectance spectrum ($BaSO_4$): 503 and 644 nm.

*$(PPh_4)_2[W(CN)_4O(O_2)]$ (**3**)*

Oxygen was bubbled through a solution of $(PPh_4)_3[W(CN)_5O] \cdot 7H_2O$ (0.5 g, 0.34 mmol) in 40 cm^3 of ethanol-acetone mixture (1:1) until the volume was reduced to 1 cm^3. The resulting white crystals were filtered off, washed with ethanol and dried in air. Yield *ca*. 80%. Selected IR bands (KBr) ν_{max}/cm^{-1}: ν(O–O) 871m; ν(W=O) 933s; ν(C≡N) 2132vvw, 2154vvw, 2199vvw. UV-Vis spectra (acetonitrile) λ_{max}/nm: 233, 263, 269, 277 and 323 (ε = 635 mol^{-1} dm^3 cm^{-1}). Reflectance spectrum ($BaSO_4$): 237, 281 and 336 nm.

Anal. Calcd. for $C_{52}H_{40}N_4O_3P_2W$: C, 61.54; N, 5.52; H, 3.94%. Found: C, 61.34; N, 5.29; H, 3.92%.

Analytical Methods and Physical Measurements

Carbon, hydrogen and nitrogen were determined by conventional organic microanalysis. Hydration water was determined by dehydration over P_4O_{10} under restricted anaerobic conditions on a vacuum line. UV-Vis absorption spectra were recorded on a Shimadzu UV 2101PC. Reflectance spectra were measured as pellets in $BaSO_4$ *vs.* $BaSO_4$ as reference (Shimadzu UV 2101PC equipped with ISR-260 attachment). IR spectra were measured as KBr pellets on a Bruker IFS 48 spectrometer. ESR spectra were measured on a Bruker ELEXSYS spectrometer at room temperature using diphenylpicrylhydrazide (dpph) as an internal standard. Thermogravimetric and differential thermal analysis were performed on a Mettler thermoanalyser TGA/SDTA 851, under argon or in air at a heating rate of 5 K per minute. Cyclic voltammetry measurements were performed in 0.1 mol dm^{-3} $(Bu_4N)PF_6$ as electrolyte in acetonitrile and ethanol using Pt working and counting and Ag/AgCl reference electrode on a Model EA9 Electrochemical Analyser (Poland). The redox potentials are reported *versus* ferrocene, which was used as an internal potential standard for measurements in organic solvents to avoid the influence of liquid junction potential. $E_{1/2}$ values were calculated from the average anodic and cathodic peak potentials, $E_{1/2} = 0.5\ (E_{pa} + E_{pc})$.

^{31}P NMR spectra of salt **3** were recorded on a Tesla BS-567A spectrometer. The reaction of salt **3** with triphenylphosphine was carried out in MeCN at 298 K under argon and/or under oxygen. The complex/PPh_3 mole ratio was 1 : 5.

The kinetic measurements were performed in ethanol-acetone mixture (1:1 volume ratio) using an Applied Photophysics Stopped Flow apparatus connected to a Shimadzu UV 2101PC spectrophotometer focused on 573 nm. The spectrophotometer was equipped with a CPS-260 temperature controller while the Stopped Flow apparatus employed a conventional water thermostat. To avoid oxidation, all manipulations were performed under anaerobic conditions using Schlenk techniques. The solvents (ethanol and acetone) were boiled for 40 minutes under argon to remove the oxygen. Complex **1** was dissolved in deaerated ethanol-acetone (1:1) mixture prior to use. The kinetics of the reaction of complex **1** with dioxygen was studied under pseudo first-order conditions using the excess of complex ([complex] = $1.2 \times 10^{-2} - 3.37 \times 10^{-2}$ mol dm^{-3}) over oxygen ($[O_2] = 2.41 \times 10^{-3}$ mol dm^{-3}). The reaction progress was followed at 573 nm (band maximum of the substrate). The pseudo first-order rate constants were obtained from plots of $\log(A_\infty - A_t)$ *versus* time, where A_t is the absorbance at time t and A_∞ is the absorbance extrapolated to $t = \infty$. The measurements were performed in the 298–313 K range; all temperatures are reported within ± 0.2 K.

The solid state kinetic measurements were performed at 323 K (± 0.2 K) using NaCl plates covered with a thin layer of salt **1**, which was transformed to salt **2** under

these conditions. The spectra (measured in absorbance mode) were collected every 30 minutes and the integrated intensities of the O–O, W=O and C≡N bands of complexes **2** and **3** were taken for kinetic calculations. The very strong band of the PPh_4^+ cation at 1107 cm^{-1} was used as an internal intensity standard.

Crystal Structure Determination of $(PPh_4)_3[W(CN)_5O] \cdot 7H_2O$

Crystals of salt **1**, suitable for X-ray crystallography, were selected from the material prepared as described above. Crystal data for salt **1**, and a summary of data

TABLE I

Crystal data and structure refinement parameters for salt **1**

Empirical formula	$C_{77}H_{74}N_5O_8P_3W$	
Formula weight	1474.17	
Temperature / K	180(2)	
Wavelength / pm	71.073	
Crystal system	Triclinic	
Space group	*P*1	
Unit cell dimensions / pm, °	a = 1237.77(15)	α = 77.617(7)
	b = 1578.85(11)	β = 84.594(13)
	c = 1899.78(16)	γ = 74.131(13)
Volume / pm^3	3485.6(6) × 10^6	
Z	2	
Density (calculated) / Mg m^{-3}	1.405	
Absorption coefficient / mm^{-1}	1.786	
F(000)	1508	
Crystal size / mm^3	0.68 × 0.62 × 0.52	
Theta range for data collection / °	2.60 to 26.50	
Index ranges	$-1 \le h \le 12$, $-18 \le k \le 19$, $-23 \le l \le 23$	
Reflections collected	14274	
Independent reflections	13496 [*R*(int) = 0.0183]	
Completeness to theta = 26.50° / %	93.4	
Absorption correction	Psi-scan	
Max. and min. transmission	0.496 and 0.388	
Refinement method	Full-matrix least-squares on F^2	
Data / restraints / parameters	13496 / 0 / 847	
Goodness-of-fit on F^2	1.049	
Final *R* indices [$I>2\sigma(I)$]	*R*1 = 0.0318, *wR*2 = 0.0669	
R indices (all data)	*R*1 = 0.0428, *wR*2 = 0.0703	
Largest diff. peak and hole / e pm^{-3}	1.978 and –0.718 × 10^{-6}	

collection and structure refinement parameters, are given in Table I. The positions of the W and P atoms were determined by Patterson methods; the remaining non-hydrogen atoms were located in successive difference Fourier syntheses. Hydrogen atoms were included in the structure factor calculations at idealised positions and were not refined. In the final refinement cycle, all non-hydrogen atoms were refined anisotropically. The largest peaks in the final difference maps were located near the W atoms. All calculations were performed using SHELXTL-pc; scattering factors and anomalous dispersion factors were those given in SHELXTL.[8] Full crystallographic data may be obtained from the Cambridge Crystallographic Data Centre, where CIF files have been deposited (Deposition Number 144778).

RESULTS

*Characterisation of Complex **1***

Salt **1** is a diamagnetic, dark green solid, stable in the solid state when kept under anaerobic conditions. It is freely soluble in ethanol and in acetonitrile; such solutions are stable for several days. The complex is insoluble in acetone but undergoes dehydration with a colour change to dark brown, without any other changes. The complex can be easily and reversibly dehydrated over P_4O_{10} in *vacuo* or dried at 323 K, with a colour change from light green to dark brown. The thermogravimetric and differential thermal analysis measurements indicate that the water molecules are weakly bonded and are released in two separate steps with T_{max} equal to 328 and 353 K. In the first process, which starts at room temperature, five water molecules are lost whereas in the second one two water molecules are released (calculated Δm for this process 2.4%, found 2.2% (in argon) and 2.3% (in air)). After dehydration, under anaerobic conditions, the complex is stable up to 433 K, while in the presence of oxygen the decomposition process starts above 373 K.

The salt undergoes irreversible oxidation at *ca.* 1608 mV in acetonitrile (100 mV s^{-1}) (Figure 1), while in ethanol-acetone (1:1) mixture the process is reversible with the oxidation potential equal to 504 mV (100 mV s^{-1}).

Structure of $(PPh_4)_3[W(CN)_5O]\cdot 7H_2O$

The cell projection of salt **1** is presented in Figure 2 and the selected bond lengths and angles are given in Table II. The salt consists of discrete anion and cation units, which are bonded by a network of hydrogen-bonds in which all water molecules are involved. There are several kinds of hydrogen-bonds (Figure 3) in the structure:

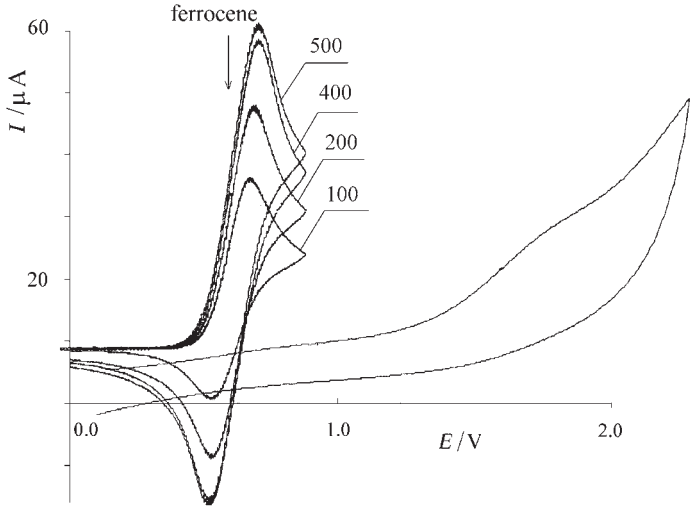

Figure 1. The cyclic voltammetry of salt **1** in acetonitrile ($c = 1 \times 10^{-3}$ mol dm^{-3}). Numbers indicate the scan speed in mV s^{-1}. Ferrocene is an internal potential standard.

(i) two water molecules [O(8) and O(5)] form a bridge between two cyano ligands of the same anion with the bond distances N(5)–O(8), O(8)–O(5) and O(5)–N(4) equal to 289.9, 284.1 and 300.0 pm, respectively;

(ii) one water molecule is hydrogen-bonded to only one cyano ligand [O(9)–N(2)] with bond length 279.9 pm;

(iii) the other water molecule is bonded to the nitrogen of a cyano ligand [N(3)–O(4), 296.4 pm] and to three remaining water oxygens [O(7), O(6) and O(10) with bond lengths O(4)–O(7), O(7)–O(10) and O(7)–O(6) equal to 281.3, 287.2 and 279.6 pm, respectively].

There is also hydrogen-bonding between anions with the O(10'')–O(3) distance 282.9 pm and the N(4)–O(5') distance 297.1 pm, with a very weak interaction O(4)–N(1) (bond distance 321.2 pm).

The $[W(CN)_5O]^{3-}$ anion has distorted octahedral symmetry. The W=O bond distance (172.4 pm) is somewhat longer than that found for its Mo analogue (170.5 pm).[4,9] The cyano ligand in the *trans* position to the oxygen [C(3)–N(3)] has the longest W–C (234.9 pm) and W–N (350.0 pm) distances, as was also found for its molybdenum analogue (with Mo–C and Mo–N distances equal to 237.3 pm and 348.7 pm). For all other cyanide ligands, the average W–C and C≡N distances are equal to 214.2 and 115.3 pm, respectively (for the molybdenum compound average Mo–C and C≡N distances are 217.8 and 113.7 pm). The angle C(3)–W–O(3) is 175.16°. The cyano ligands in the equatorial plane are shifted away from the oxygen atom at an average

TABLE II

Selected bond lengths and angles for salt **1**

Bond lengths / pm			
W(1) – O(1)	172.4(2)	C(1) – N(1)	115.7(4)
W(1) – C(5)	213.4(3)	C(2) – N(2)	114.9(4)
W(1) – C(2)	214.3(3)	C(3) – N(3)	115.1(4)
W(1) – C(1)	214.5(3)	C(4) – N(4)	115.3(4)
W(1) – C(4)	214.6(3)	C(5) – N(5)	115.3(4)
W(1) – C(3)	234.9(4)		
Hydrogen bond lengths / pm			
N(3) – O(4)	296.4	N(5) – O(8)	289.9
N(2) – O(9)	279.9	N(4) – O(5)	300.0
O(4) – O(7)	281.3	N(4) – O(5′)	297.1
O(7) – O(6)	279.6	O(3) – O(10″)	282.9
O(8) – O(5)	284.1	O(7) – O(10)	287.2
Selected bond angles / °			
O(3) – W(1) – C(5)	100.06(12)	O(3) – W(1) – C(3)	175.16(11)
O(3) – W(1) – C(2)	100.98(12)	C(5) – W(1) – C(3)	78.83(12)
C(5) – W(1) – C(2)	158.78(12)	C(2) – W(1) – C(3)	80.42(12)
O(3) – W(1) – C(1)	97.48(12)	C(1) – W(1) – C(3)	77.90(12)
C(5) – W(1) – C(1)	91.92(12)	C(4) – W(1) – C(3)	82.38(12)
C(2) – W(1) – C(1)	88.06(12)	N(1) – C(1) – W(1)	178.9(3)
O(3) – W(1) – C(4)	102.26(12)	N(2) – C(2) – W(1)	178.4(3)
C(5) – W(1) – C(4)	85.12(12)	N(3) – C(3) – W(1)	175.3(3)
C(2) – W(1) – C(4)	87.77(12)	N(5) – C(5) – W(1)	176.1(3)
C(1) – W(1) – C(4)	160.26(12)	N(4) – C(4) – W(1)	178.0(3)

Symmetry codes: ′ $-x, -y, 1-z$ and ″ $1+x, y, z$.

O(3)–W–C angle of 100.2° compared to C(3)–W–C equal to 79.9°. Identical values were found for the molybdenum analogue (100.2° and 79.9°, respectively).

*Reaction of Salt **1** with Molecular Oxygen*

In oxygenated ethanol-acetone mixture (1:1 volume ratio), a fast change from green to colourless is observed. The product of this reaction has been isolated as salt **3**, formed according to the overall reaction stoichiometry:

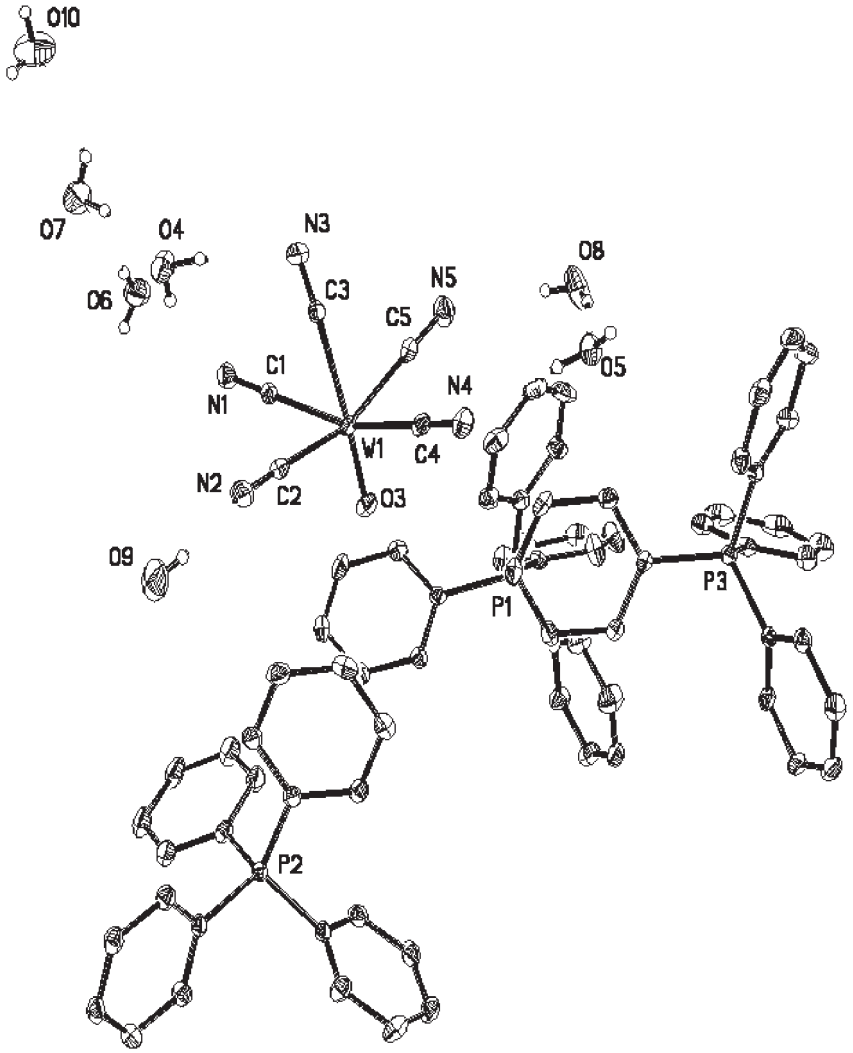

Figure 2. The molecular structure of $(PPh_4)_3[W(CN)_5O] \cdot 7H_2O$. Displacement parameters are shown at the 30% level and phenyl H atoms are omitted for clarity.

$$[W(CN)_5O]^{3-} + O_2 \rightarrow [W(CN)_4O(O_2)]^{2-} + CN^- \quad (1)$$

The formal oxidation state of tungsten is VI and salt **3** is diamagnetic. The same product, but mixed with $(PPh_4)CN$, can be obtained when the solid salt **1** is kept in air for a long time (*ca.* one month). To obtain pure salt, it has to be recrystallised from ethanol. The elemental analysis, IR data, and

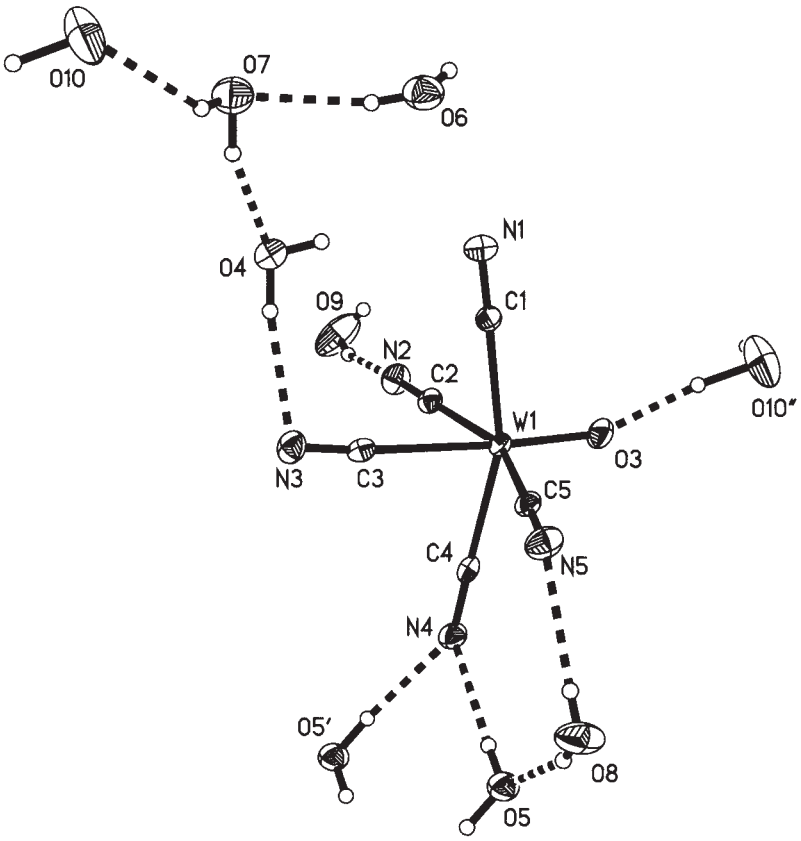

Figure 3. The structure of $[W(CN)_5O]^{3-}$ anion showing the hydrogen bonds (dashed lines).

UV-Vis spectra (both in solution and in the solid state) are identical with those of the $(PPh_4)_2[W(CN)_4O(O_2)]$ formed in the reaction of $(PPh_4)_2[W(CN)_4O(pz)] \cdot 3H_2O$ with dioxygen.[6] Salt **3** is white, readily soluble in acetone, dichloromethane and acetonitrile but almost insoluble in ethanol, methanol and water. It is stable in air for long periods of time.

*Reaction of Salt **3** with Triphenylphosphine*

It is known that the molybdenum peroxo complex reacts with triphenylphosphine in acetonitrile, oxidising it to the phosphine oxide. The ^{31}P NMR spectra of the solution of complex **3** in acetonitrile in the presence of triphenylphosphine indicate that, under an inert atmosphere, one mole of triphenylphosphine oxide per mole of complex is produced. In oxygenated solution,

the stoichiometry 1:1 is also maintained. Thus, the observed reaction can be written as

$$[W(CN)_4O(O_2)]^{2-} + Ph_3P \rightarrow [W(CN)_4(O)_2]^{2-} + Ph_3PO \quad (2)$$

The Solid State Reaction of Salt **2** *with Dioxygen*

The progress of this solid state reaction was followed by measuring IR spectra. The representative vibrations for salts **2** and **3** are shown in Figure 4. The results of IR measurements of complex **2** kept in air at 323 K show that the formation of complex **3** is a complicated process. During the reaction with dioxygen (Figure 5), the integrated intensity of the bands at 871, 917, 930, 2060 and 2068 cm^{-1} changes with time according to the first-order kinetics. The values of k_{ex} calculated from the plot of $\log(A_\infty - A_t)$ *versus*

TABLE III

The kinetic data of the reaction of salt **2** with dioxygen in the solid state

ν / cm^{-1}	Band	$10^4\, k_{ex}$ / s^{-1}
871	O–O	1.72 ± 0.04
917	W=O in salt **1**	3.3 ± 0.3
930	W=O in salt **2**	2.5 ± 0.1
2060	C≡N	5 ± 1
2068	C≡N	47 ± 2

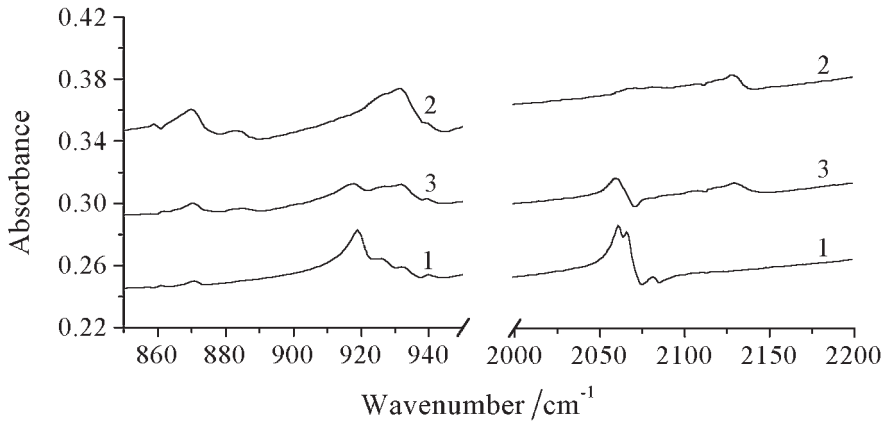

Figure 4. Selected IR bands of salts **2** (curve 1) and **3** (curve 2) together with the spectrum of salt **2**, reacting with oxygen at 323 K recorded after 30 minutes (curve 3).

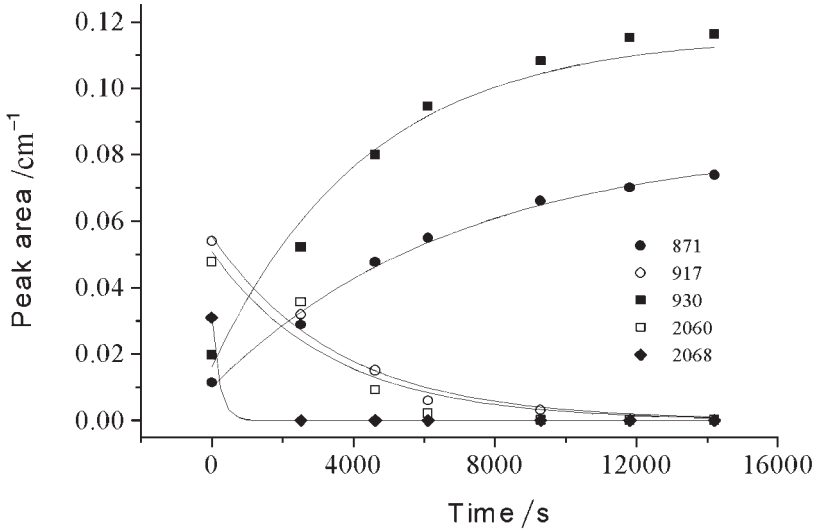

Figure 5. Changes in the peak areas of selected bands in the IR spectrum of salt **2** *versus* time.

time (where A_∞ is the band area at infinite time, A_t is the band area at time t) are given in Table III. It can be seen from Figure 5 and Table III that the intensity of one of the C≡N bands rapidly decreases ($k_{ex} = 47 \times 10^{-4}$ s^{-1}), whereas the other decreases at a rate ($k_{ex} = 5 \times 10^{-4}$ s^{-1}) similar to that of the W=O band shift (from a position typical of salt **2** to that of salt **3**). The slowest process is O–O bond formation ($k_{ex} = 1.72 \times 10^{-4}$ s^{-1}).

*Kinetics of the Reaction of Salt **1** with Molecular Oxygen in Solution*

When salt **1** is dissolved in a deaerated ethanol-acetone mixture and the solution is left open to the air, the solution slowly changes colour from green to yellow; the spectral changes are shown in Figure 6. This process is connected with 1 mole of oxygen uptake per 1 mole of salt **1**. The yellow solution can be kept under argon for several hours without change, however, the presence of oxygen converts the yellow intermediate into salt **3**. This has low solubility in ethanol-acetone mixture and starts to crystallise, resulting in an absorption increase without any specific maximum. The ESR spectrum (Figure 7) of the yellow solution indicates the presence of a d^1-W(V) compound, whose amount increases with increasing intensity of the yellow colour. The excess of oxygen results in decay of the yellow compound, accompanied by a decrease of the ESR signal, which may be ascribed to the formation of a diamagnetic W(VI) complex **3**.

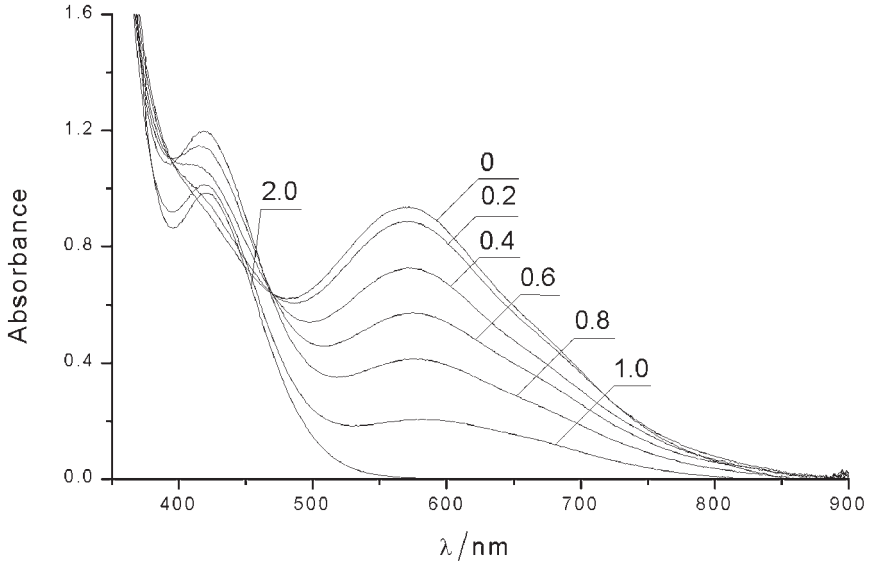

Figure 6. Spectral changes of the solution of salt **1** in ethanol-acetone mixture (1 : 1) with added oxygen. Numbers indicate the moles of oxygen per mole of salt **1**. (c = 0.012 mol dm^{-3}, d = 1 cm).

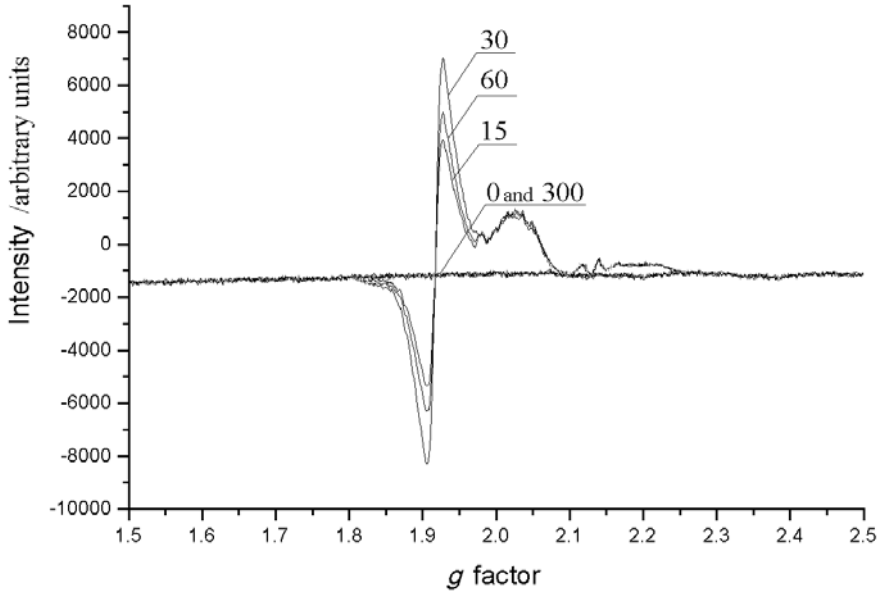

Figure 7. The ESR spectrum of salt **1** in partially oxygenated ethanol-acetone (1 : 1) solution in a holder open to air. Numbers indicate the time (in minutes) after which the spectra were recorded.

The reaction kinetics under the conditions of an excess of complex over oxygen results in the formation of a new band at 423 nm, attributed to the yellow intermediate. The reaction was found to be of the first order in oxygen concentration by the rate law

$$-\mathrm{d[complex]}/\mathrm{d}t = k_{obs}[O_2] \quad (3)$$

The value of k_{obs} is equal to 0.0479 s^{-1} (T = 298 K, complex / oxygen ratio = 5 : 1).

The k_{obs} was found to be linearly dependent on the concentration of $[W(CN)_5O]^{3-}$ (Figure 8) and can be expressed by the equation

$$k_{obs} = k[\mathrm{complex}] \quad (4)$$

The values of k at different temperatures are collected in Table IV. The activation parameters $\Delta H^{\ddagger}$ (k) and $\Delta S^{\ddagger}$ (k) were found to be equal to 55 (±3) kJ mol^{-1} and –46 (±8) J K^{-1} mol^{-1}.

TABLE IV

The kinetic data for the reaction of salt **1** with dioxygen in ethanol-acetone (1 : 1) mixture

T / K	298	303	306	308	311	313
k / mol^{-1} dm^3 s^{-1}	5.78 ± 0.26	8.01 ± 0.23	9.71 ± 0.29	11.47 ± 0.39	14.83 ± 0.50	17.19 ± 0.63
$\Delta H^{\ddagger}$ / kJ mol^{-1}			55 ± 3			
$\Delta S^{\ddagger}$ / J K^{-1} mol^{-1}			–46 ± 8			

The Reaction Mechanism

Despite the simplicity of the second-order rate law and of the 1:1 stoichiometry, it is very difficult to propose a mechanism consistent with all the experimental data detailed above and valid both for the solid state and in solution. The complexity of the system means that the observed kinetics can be only interpreted in a qualitative way. However, our results indicate that the reaction proceeds *via* three main stages:

$$A + O_2 \xrightarrow{fast} I_1 + X \quad (5)$$

$$I_1 + O_2 \xrightarrow{slow} I_2 \quad (6)$$

$$I_2 \xrightarrow{fast} P + O_2 \quad (7)$$

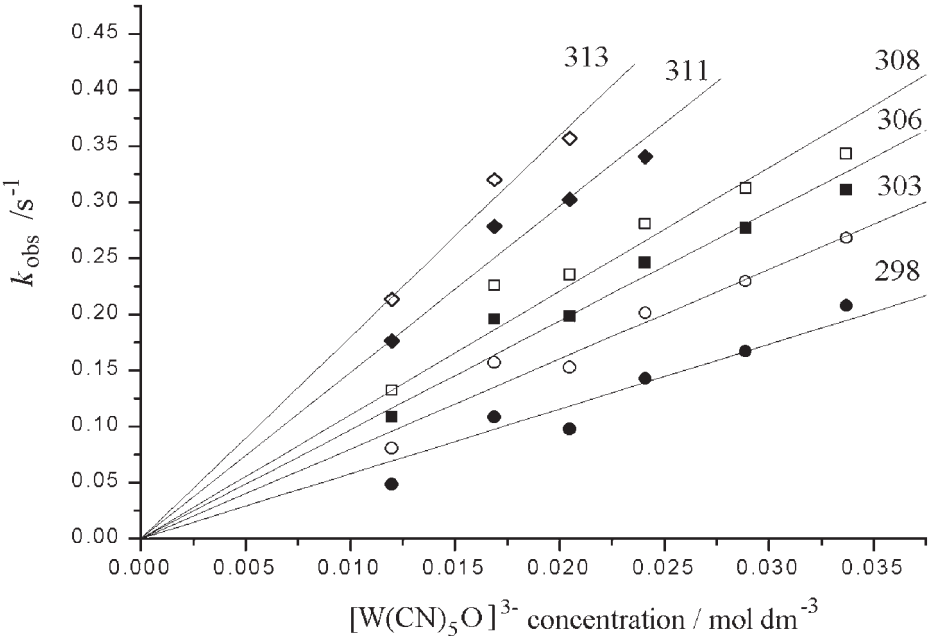

Figure 8. The plot of k_{obs} *versus* concentration of $[W(CN)_5O]^{3-}$. Numbers indicate the temperature in K.

In the first stage, the $[W(CN)_5O]^{3-}$ anion (A) reacts with dioxygen, giving the yellow intermediate (I_1), which we suppose to be $[W^V(CN)_4O(O_2)]^{2-}$ with an end-on bonded superoxo group coordinated to tungsten(V). This step involves a nucleophilic attack by O_2, release of cyanide (X), and electron transfer from W^{IV} to the O_2. All these processes are relatively fast. The release of cyanide and the electron transfer are responsible for the rapid disappearance of one of the cyanide bands, that at 2068 cm^{-1}, from the IR spectrum. It is known that the cyanide bands are of lower intensity for tungsten(V) complexes and still lower for tungsten(VI). The ESR spectra in solution support the formation of a paramagnetic W^V compound. Unfortunately, we cannot see the O_2^- band at about 1100 cm^{-1} as this is covered by the strong band of the PPh_4^+ cation at 1107 cm^{-1}.

In the second stage, I_1 reacts with the other molecule of dioxygen (if there is a lack of oxygen the reaction proceeds more slowly) giving I_2, which we suppose to be $[W^{VI}(CN)_4O(O_2)_2]^{2-}$ with two superoxo groups in *cis* positions. This process seems to be a rate limiting step and should be associatively activated (I_a or A), as results from the negative value of $\Delta S^{\ddagger}$ (k). The last stage leads to the peroxo compound of tungsten(VI) through cleavage of

the superoxo bonds with a concomitant release of O_2 and formation of the oxygen-oxygen bond in the side-on peroxide ligand

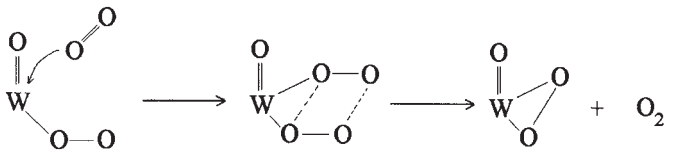

Partial oxygen-oxygen bond formation in the potential leaving O_2 molecule can compensate for the necessary stretching of two fairly strong O–O bonds in the superoxide ligands in the four-centre transition state or the transient intermediate shown above. It should be admitted that four-centre transition states are by no means uncommon. A similar mechanism was proposed for *e.g.* reaction of tin(IV) alkyls with mercury(II) halides[10a] or for certain classes of insertion and elimination reactions in organometallic chemistry.[10b] In the present system, a significant constraint is introduced by the coordination of two of the centres to the tungsten.

An extensive programme of further experiments would be required on heptahydrate, on anhydrous material and in solution to establish whether a common mechanism applies all three situations and to indicate an unequivocal mechanism for this system.

Acknowledgements. – This work was supported in part by the Polish Research Grants Committee, KBN, No. 3T09A 057 17. The authors are grateful to Prof. J. Datka for valuable discussions.

REFERENCES

1. M. Dudek and A. Samotus, *Transition Met. Chem*. **10** (1985) 271–274.
2. (a) S. S. Basson, J. G. Leipoldt, I. M. Potgieter, and A. Roodt, *Inorg. Chim. Acta* **103** (1985) 121–125. (b) J. G. Leipoldt, R. van Eldik, S. S. Basson, and A. Roodt, *Inorg. Chem.* **25** (1986) 4639–4642. (c) J. P. Smit, W. Purcell, A. Roodt, and J. G. Leipoldt, *J. Chem. Soc., Chem. Commun.* (1993) 1388–1389.
3. (a) J. G. Leipoldt, S. S. Basson, A. Roodt, and I. M. Potgieter, *S. Afr. J. Chem.* **39** (1986) 179–183. (b) I. M. Potgieter, S. S. Basson, A. Roodt, and J. G. Leipoldt, *Transition Met. Chem.* **13** (1988) 209–211. (c) A. Roodt, J. G. Leipoldt, S. S. Basson, and I. M. Potgieter, *Transition Met. Chem*. **13** (1988) 336–339.
4. H. Arzoumanian, J. F. Petrignani, M. Pierrot, F. Ridouane, and J. Sanchez, *Inorg. Chem*. **27** (1988) 3377–3381.
5. H. Arzoumanian, M. Pierrot, F. Ridouane, and J. Sanchez, *Transition Met. Chem*. **16** (1991) 422–426.
6. D. Matoga, J. Szklarzewicz, A. Samotus, J. Burgess, J. Fawcett, and D. R. Russell, *Polyhedron* **19** (2000) 1503–1509.

7. A. Roodt, S. S. Basson, and J. G. Leipoldt, *Polyhedron* **13** (1994) 599–607.
8. G. M. Sheldrick, SHELXTL-pc Release 4.2, Siemiens Analytical X-Ray Instruments, Madison, WI, 1991.
9. K. Wieghardt, G. Backes-Dahmann, W. Holzbach, and W. J. Swiridoff, *Z. Anorg. Allg. Chem.* **499** (1983) 44–58.
10. (a) M. L. Tobe and J. Burgess, *Inorganic Reaction Mechanism*, Addison-Wesley-Longman, Harlow, 1999, p. 64; (b) pp. 586 and 603.

SAŽETAK

Struktura i reaktivnost $(PPh_4)_3[W(CN)_5O] \cdot 7H_2O$. Kinetika i mehanizam reakcije s molekulnim kisikom

Janusz Szklarzewicz, Dariusz Matoga, Alina Samotus, John Burgess, John Fawcett i David R. Russell

Kompleksni spoj $(PPh_4)_3[W(CN)_5O] \cdot 7H_2O$ sintetiziran je i karakteriziran s pomoću difrakcije X-zraka. U čvrstom stanju i u smjesi etanol-aceton spoj reagira s molekulnim kisikom, dajući $(PPh_4)_2[W(CN)_4O(O_2)]$. Doseg reakcije u čvrstom stanju praćen je mjerenjem infracrvenog spektra. Vremenska promjena integriranih inteziteta vrpci W=O, O–O i CN u skladu je s kinetikom pseudoprvog reda. Kinetička mjerenja u otopini pokazuju slijedeći izraz za brzinu reakcije: $-d[\text{kompleks}] / dt = k[\text{kompleks}][O_2]$.

Brzina reakcije iznosi $(5{,}78 \pm 0{,}26)$ mol^{-1} dm^3 s^{-1}. Aktivacijski parametri su $\Delta H^{\ddagger}(k) = (55 \pm 3)$ kJ mol^{-1} i $\Delta S^{\ddagger}(k) = -(46 \pm 8)$ J K^{-1} mol^{-1}. Predložen je mehanizam reakcije.